

EDLC performance of carbide-derived carbons in aprotic and acidic electrolytes

J.A. Fernández^a, M. Arulepp^b, J. Leis^c, F. Stoeckli^d, T.A. Centeno^{*a}

^a*Instituto Nacional del Carbón-CSIC. Apartado 73. 33080 Oviedo, Spain*

^b*Tartu Technologies Ltd., 185 Riia Str., 51014 Tartu, Estonia*

^c*University of Tartu, 2 Jakobi Str. 51014 Tartu, Estonia*

^d*IMT-Chimie des Surfaces, Université de Neuchâtel. Rue Emile Argand 11, CH-2009 Neuchâtel, Switzerland*

Abstract

This study shows that carbide-derived carbons (CDCs) with average pore size distributions around 0.9 to 1 nm and effective surface areas of 1300-1400 m² g⁻¹ provide electrochemical double layer capacitors with high performances in both aqueous (2M H₂SO₄) and aprotic (1M (C₂H₅)₄NBF₄ in acetonitrile) electrolytes.

In the acidic electrolytic solution, the gravimetric capacitance at low current density (1 mA cm⁻²) can exceed 200 F g⁻¹, whereas the volumetric capacitance reaches 90 F cm⁻³. In the aprotic electrolyte they reach 150 F g⁻¹ and 60 F cm⁻³.

A detailed comparison of the capacitive behaviour of CDCs at high current density (up to 100 mA cm⁻²) with other microporous and mesoporous carbons indicates better rate capabilities for the present materials in both electrolytes. This is due to the high surface area, the accessible porosity and the relatively low oxygen content.

It also appears that the surface related capacitances of the present CDCs in the aprotic electrolyte are in line with other carbons and show no anomalous behaviour.

Keywords: Electrical double-layer capacitor, carbide-derived carbon, porosity

* Corresponding author, Tel.: +34 985119090; Fax: +34 985297662;
E-mail address: teresa@incar.csic.es (T.A. Centeno)

1. Introduction

The optimisation of electrochemical double layer capacitors (EDLCs) is critical for the next generation of electrical energy storage systems. As far as the performance of these devices depends greatly on the properties of their material electrodes, the development of innovative carbons to maximize the energy-power density lies at the centre of future breakthroughs for larger scale implementation [1-4].

Many carbons with a variety of porous structures and surface chemistries have been evaluated as electrode materials for electrochemical capacitors [3-5]. The origin of the high performances of certain carbons remains a matter of debate and an appropriate description can be of help for the preparation of materials with optimum properties. In the case of typical activated carbons with pores above 0.65-0.70, their performance in the aprotic electrolyte 1M $(\text{C}_2\text{H}_5)_4\text{NBF}_4$ in acetonitrile seems to correspond basically to a linear dependence between the specific capacitance and the specific surface area as a consequence of an electrical double-layer mechanism [6]. Carbons which do not follow this trend in aprotic electrolytes tend to be materials with average pore widths below 0.75-0.80 nm [6]. For some carbons, the specific capacitance in the aqueous H_2SO_4 electrolyte also appears to include a faradaic contribution as well as an electrostatic component. Thus, the specific capacitance consists of a contribution from the total accessible surface area and of an additional pseudo-capacitance based on certain surface functionalities, such as oxygenated species and nitrogen-containing groups [7-9].

Several studies have suggested that novel carbons with high specific surface areas and with narrow pore size distributions centered in the mesopore range (2 to 50 nm) could be potentially more advantageous than microporous carbons (also called nanoporous carbons and having pore sizes up to 2 nm) [9-11]. Indeed, mesoporous carbons obtained by the templating technique [12] or by the carbonization of mixtures of poly(vinyl alcohol) with magnesium citrate [13] essentially perform as electrochemical double layer capacitors

through the extent of their total surface area and they are well adapted for high charge/discharge loads in aqueous and aprotic media.

Carbon nanotubes generally have low specific capacitances as a result of their low specific surface area. Although etching or specific post-treatments have increased their performance significantly, these materials are still less competitive than other carbons [3]. Recently, a new group of microporous carbon materials obtained by chlorination of metal carbides (carbide-derived carbons, CDCs) have been considered as excellent candidates for EDLC electrodes [14-17]. CDCs present high specific surface areas and tunable pore sizes by controlling the chlorination temperature and/or by the choice of the raw carbide [18-20].

The present work confirms the suitability of carbide-derived carbons for electrochemical capacitors, by comparing their performances with those of other porous carbon materials under the same experimental conditions. However, it would appear that for the present CDCs with average pore sizes as low as 0.9 nm and a fraction of smaller pores, the surface related capacitance is similar to that of other carbons [6-8, 12-13]. The study also provides an insight into the limits of EDLC systems based on carbons in general.

2. Experimental

Our study is based on four carbide-derived carbons produced from SiC, TiC/SiC, TiC/TiO₂, and TiC. Their synthesis was performed by extracting of the metal from carbide powders in the flow of chlorine at high temperature [20]. This process is generally described by the equation:



The SiC-based carbon was obtained at 1000°C. The TiC/SiC-carbon derived from the heat treatment at 900°C of a mixture TiC and SiC powders (ratio 1:1). The TiC/TiO₂-carbon was prepared from TiC mixed with 10%(wt.) of TiO₂ and subsequent heating at 800°C. The TiC-derived carbon was obtained by stepwise chlorination at 950°C and 800°C

[20]. To avoid the oxidation of the CDC powder during production, the inert atmosphere was maintained before and after the chlorination process.

All CDC materials were treated in hydrogen at 800°C to passivate the highly reactive dangling bonds and also to purify the carbons by removing chlorides.

The porous structure of the carbons was analysed by N₂ adsorption at 77 K (*Micromeritics ASAP 2010*) and the enthalpies of immersion were carried out as described elsewhere [7, 8]. The low pressure data for nitrogen adsorption was analyzed within the framework of Dubinin's theory, which leads to S_{mi} , the surface area of the ideally slit-shaped micropores. On the other hand, the comparison of the overall isotherm with adsorption on the non-porous reference carbon black Vulcan-3G [8, 21], leads to both the total surface area S_{comp} and the external (non-microporous) area S_e . The latter can also be determined independently, either by immersion calorimetry or by the preadsorption of nonane in the nanopores at room temperature, followed by the nitrogen isotherm at 77 K on S_e . As shown in Table 1 and observed for other carbons, the total surface area $S_{tot} = S_{mi} + S_e$ and S_{comp} are in good agreement (It is also found that they usually agree with the surface area obtained from the adsorption of phenol from aqueous solutions [6,7,22]). On the other hand, as discussed elsewhere [22], S_{BET} tends to overrate the surface area in micropores above 0.9 to 1 nm, where it corresponds to the monolayer equivalent of the pore volume (2220 m² per cm³). The surface-related properties reported here are calculated on the basis of $S_{tot} = S_{mi} + S_e$. Further information on the accessibility of the micropore system has been obtained from the enthalpies of immersion into C₆H₆ ($\Delta_iH(C_6H_6)$) and CCl₄ ($\Delta_iH(CCl_4)$), liquids with molecular dimensions of respectively 0.41 nm (flat molecule) and 0.65 nm (spherical molecule) [7-8].

As opposed to organic liquids, where the volume filling of micropores is the fundamental process, water interacts strongly with functional groups of carbon surface (mainly oxygen-containing groups). It follows that the comparison of the enthalpies of immersion into water and benzene allows estimating the oxygen content of the carbon surface [7, 8]. The

results are usually in good agreement with the oxygen contents determined by TPD (thermally programmed desorption) [23, 24].

The electrochemical performance has been tested in a sandwich-type capacitor. It was set up with two carbon pellets (8 mm in diameter, around 350 μm in thickness) separated by glassy fibrous paper (300 μm in thickness) and placed inside a Swagelok-cell. The electrodes were obtained by pressing a mixture of the carbon (75 %wt), polyvinylidene fluoride (20 %wt) as binder and carbon black (Super P, 5 %wt). The electrolytes were 2M H_2SO_4 aqueous solution and 1M $(\text{C}_2\text{H}_5)_4\text{NBF}_4$ in acetonitrile. The charge storage properties were tested by galvanostatic charge-discharge voltage cycles (potentiostat-galvanostat *Autolab-Ecochimie PGSTAT 30*) at current densities, j , between 1 and 100 mA cm^{-2} in the range 0 V - 0.8 V for the aqueous electrolyte and 0 V - 2 V in the aprotic solution. The limiting capacitances measured at 1 mA cm^{-2} are respectively $C_{\text{o-aprotic}}$ and $C_{\text{o-acidic}}$. The gravimetric capacitance (F g^{-1}) given in the present study is relative to the carbon mass in a single electrode, whereas the volumetric capacitance (F cm^{-3}) is based on the electrode volume.

Energy- and power-density of the capacitors were estimated from the discharge step in the constant current measurements. Both parameters are relative to the carbon mass in the capacitor cell.

3. Results and discussion

The main structural and electrochemical characteristics of the CDC materials discussed below are given in Tables 1 and 2.

In the case of the SiC- and TiC/SiC-derived carbons the analysis reveals similar microporous systems with micropore volumes close to $0.6 \text{ cm}^3\text{g}^{-1}$, average micropore widths around 0.9 nm and microporous surface areas S_{mi} of approximately $1280 \text{ m}^2\text{g}^{-1}$.

On the other hand, it appears that the TiC- and TiC/TiO₂ derived carbons form a different group with a somewhat larger structure, which illustrates the effect of the precursors on the

resulting CDCs. The micropore volume W_0 increases to 0.73-0.75 cm³ g⁻¹, the average micropore size shifts to approximately 1.03 nm and the total surface area exceeds 1400 m² g⁻¹. Beside micropores, the present CDCs present some meso- and macroporosity but the comparison with the non-porous carbon black *Vulcan-3G* indicates low external (non-microporous) surface areas S_{ext} which do not exceed 50 m² g⁻¹ (Table 1).

The total surface areas of the present CDCs are in the range of 1300 to 1400 m²g⁻¹. They compare well with the upper-bound values found for highly porous carbons such as activated carbons [7, 8] and for mesoporous carbons obtained by more complex procedures (For example, templating techniques [12] or the carbonization of thermoplastic polymers with MgO precursors [13] with areas up to 1300 m² g⁻¹).

Moreover, the same surface areas are accessible to both acidic and aprotic electrolytes even for the SiC and TiC/SiC based carbons with average micropore sizes of 0.90 and 0.94 nm. As shown earlier [15, 16], the DFT-based pore size distributions indicate a sharp drop around 0.6 to 0.7 nm, which suggests that there are no pores below this size. Moreover, the ratios of the enthalpies of immersion into CCl₄ and C₆H₆ (Table 1) are close to 0.96, the value expected for equal accessibility of the micropores to both liquids [25]. This confirms that the same surface area is accessible to nitrogen, benzene, CCl₄ and the different electrolytes (Carbon tetrachloride, with a critical diameter of approximately 0.65 nm, is obviously a convenient analogue for the (C₂H₅)₄N⁺ ion (0.68 nm) [14]).

The surfaces of the CDCs contain small amounts of oxygen, which can be estimated from the experimental enthalpies of immersion into water and into benzene [26]. This feature can also be illustrated by the low values of the specific enthalpies of immersion into water, $h_i(\text{H}_2\text{O}) = \Delta_i H[\text{H}_2\text{O}] / S_{\text{total}}$, which varies between -0.020 to -0.049 J m⁻² (Table 1). The lowest value corresponds practically to a carbon without surface oxygen. On the other hand, in the case of carbons based on oxygen-containing fibers or KOH-activated carbons, h_i can be as high as -0.110 J m⁻² [8, 27, 28].

Although recent papers [14, 17] have reported an anomalous increase in capacitance for carbons with pores smaller than 1 nm, the experimental results of the present work indicate no significant change in the specific capacitances (in F m^{-2}) of the CDCs with respect to other carbons, when investigated by the same experimental protocols. As shown in Table 2, the limiting capacitances $C_{\text{o-aprotic}}$ related to the total surface areas are in the range of 0.09 to 0.11 F m^{-2} , which corresponds to the typical values reported for activated carbons [6, 28].

This is also illustrated by Figure 1 which shows the dependence of the limiting gravimetric specific capacitance in $(\text{C}_2\text{H}_5)_4\text{NBF}_4/\text{CH}_3\text{CN}$ with the total specific surface area for a variety of carbons. It can be seen that the relatively high electrical double layer capacitance of CDCs is due to its surface area and it fits into the general trend proposed for microporous carbons [6, 28] characterized and tested under the same experimental conditions.

The relatively low oxygen content of the CDCs is also reflected in the case of the aqueous electrolyte (Table 2 and Figure 2). Their surface-related capacitances, which vary between 0.114 to 0.148 F m^{-2} are in good agreement with the values observed for carbons with low oxygen and ash contents [6-8]. They correspond to a lower bound defined by the dotted line with a slope of approximately 0.12 F m^{-2}). The significant contribution of the surface oxygen to the capacitance is revealed by values of $C_{\text{o-aprotic}}$ which can be as high as 0.250 F m^{-2} for oxidized carbons or carbons derived from oxygen-rich fibres. However, for these materials the gravimetric capacitance often remains in the range of 130 to 150 F g^{-1} , due to the fact that their surface does not exceed 700 to 900 $\text{m}^2 \text{g}^{-1}$ (Remarkable exceptions are KOH-activated materials such as Maxsorb [7, 8] with effective areas up to 1300 $\text{m}^2 \text{g}^{-1}$). On the other hand, the good gravimetric capacitance of the CDCs in the acidic electrolyte is a consequence of their relatively high surface areas.

As already reported [15], the high electrical conductivity of CDC materials leads to a small current-dependency of capacitance. Moreover, the low oxygen content of the

carbide-derived carbons presents a technological advantage, as it reduces the rapid decrease in C with increasing current density, j , observed for carbons with oxygen-rich surfaces [7, 8]. As discussed in detail elsewhere [6-8], the decrease of $C(j)$ in both aprotic and acidic electrolytes depends mainly on the surface complexes generating CO_2 in TPD and to some extent on the average micropore width. This is illustrated by Figure 3, showing the variation of the ratio $C(j)/C_0$ with j for the present CDC materials, the activated carbons AU-46, MX-3 and Maxsorb with average micropore size of respectively 0.84, 1.2 and 2.0 nm, and a mesoporous carbon with a narrow pore size distribution centered around 6 nm and a low oxygen content [13]. The strong decrease in $C(j)$ observed for Maxsorb reflects its high oxygen content.

Moreover, as seen in Table 2, for all CDCs the ratios $C(j)/C_0$ for $j = 50 \text{ mA cm}^{-2}$ vary between 0.8 and 0.9 in both electrolytes. The lowest value (0.77), observed for the TiC/TiO₂ carbon in the acidic electrolyte, reflects its somewhat higher surface oxygen content indicated by $h_i(\text{H}_2\text{O}) = -0.049 \text{ J m}^{-2}$.

The relatively high gravimetric capacitances C_0 and the slower decrease of $C(j)$ of the CDCs have a direct influence on the performances of the corresponding capacitors. This is reflected in the Ragone-type plots displayed in Figure 4, which includes the comparison with typical activated carbons commercialized for supercapacitor systems and the mesoporous carbon [13] of Fig. 3. The data was obtained with laboratory-scale devices and it is likely that the performance would be improved by using a commercial setup [16]. Obviously, there may be numerical changes, depending on the electrode characteristics (for example its composition, thickness, etc.), the electrolytic solutions and capacitor configuration [29], but the relative performances of the carbons can be derived from their behaviour under the same given experimental conditions.

At this stage it should also be pointed out that approaches based on the gravimetric capacitance (in F g^{-1}) can be misleading in the development of small and compact electric power sources. In this context, the volumetric capacitance referred to the electrode volume

(in F cm^{-3}) is more relevant in order to establish a coherent picture of the industrial potentiality of the different carbon materials.

The present study also confirms that the higher density of microporous carbons such as CDCs makes them much more competitive than mesoporous carbons in terms of volumetric capacitance. As illustrated by Figures 5 and 6, carbons with pore sizes around 0.9-1.0 nm reach values as high as 60 and 110 F cm^{-3} , respectively in the aprotic and aqueous electrolytes. On the other hand, the wider porosity of mesoporous materials leads to a drop to around 20 F cm^{-3} in both media.

The data obtained in the present study confirms the potential of the carbide-derived carbons in the aprotic electrolyte as far as they achieve the highest volumetric capacitance. Moreover, the gravimetric capacitance largely exceeds the value found for typical activated carbons. The capacitances of CDCs in the aqueous electrolyte are only surpassed by some activated carbons with high oxygen content and, consequently, with a significant pseudocapacitive contribution to the overall capacitance. However, in this case, the capacitance shows a faster decrease with increasing current density, j .

Finally, it should be pointed out that the good cycling stability of CDC materials has already been reported by Arulepp et al. [29]. It is a fundamental requirement for industrial applications.

4. Conclusions

In summary, CDCs with narrow pore size distributions around 0.9-1 nm and relatively high surface areas ($1300\text{-}1400 \text{ m}^2 \text{ g}^{-1}$) optimize the performance of electrochemical double layer capacitors in aqueous (2M H_2SO_4) and aprotic (1M $(\text{C}_2\text{H}_5)_4\text{NBF}_4$ / acetonitrile) electrolytes. The specific capacitance of CDCs at low current density (1 mA cm^{-2}) can exceed 200 F g^{-1} in 2M H_2SO_4 aqueous solution and it reaches 150 F g^{-1} in the aprotic medium $(\text{C}_2\text{H}_5)_4\text{NBF}_4$ /acetonitrile. Furthermore, their high volumetric capacitance (around 90 and 60 F cm^{-3} in the aqueous and the aprotic electrolytes, respectively, makes them of

great interest for application at industrial scale, where the actual volume of the device plays a role. This property, is due to the favourable surface to volume ratio in narrow pores. On the other hand, is worth pointing out that the surface related capacitance of the present CDCs in the aprotic medium (0.087 to 0.107 F m⁻²) is similar to that obtained for other nanoporous carbons by using the same protocols for the structural and the electrochemical characterizations. This observation suggests that there is no anomalous behaviour [14] for the present CDCs with average pore widths as low as 0.90 nm and pores below this value, accessible to CCl₄.

As a result of their purity, the performance of the carbide-derived carbons is essentially based on a double layer mechanism. This also reduces the significant decrease of the capacitance observed for carbons with high surface oxygen contents. As shown by the Ragone-type plots, the EDLC behaviour of carbide-derived carbons at high current density competes with that observed for commercial activated carbons developed for supercapacitors and confirms the potential of the carbide-derived carbons in high performance devices.

REFERENCES

- [1] A. Burke, *J. Power Sources* 91 (2000) 37.
- [2] R. Kötz, M. Carlen, *Electrochim. Acta* 45 (2000) 2483.
- [3] A.G. Pandolfo, A.F. Hollenkamp, *J. Power Sources* 157 (2006) 11.
- [4] A. Burke, *Electrochim. Acta* 53 (2007) 1083.
- [5] E. Frackowiak, F. Béguin, *Carbon* 39 (2001) 937.
- [6] T.A. Centeno, M. Hahn, J.A. Fernández, R. Kötz, F. Stoeckli, *Electrochem. Commun.* 9 (2007) 1242.
- [7] T.A. Centeno, F. Stoeckli, *Electrochim. Acta* 52 (2006) 560.
- [8] T. A. Centeno, F. Stoeckli, in: V. Gupta (Ed.), *Recent Advances in Supercapacitors*, Transworld Research Network, Kerala, 2006, pp. 57.
- [9] E. Frackowiak, G. Lota, J. Machnikowski, C. Vix-Guterl, F. Béguin, *Electrochim. Acta* 51 (2006) 2209.
- [10] H.Y. Liu, K.P. Wang, H. Teng, *Carbon* 43 (2005) 559.
- [11] T. Morishita, Y. Soneda, T. Tsumura, M. Inagaki, *Carbon* 44 (2006) 2360.
- [12] M. Sevilla, S. Álvarez, T.A. Centeno, A.B. Fuertes, F. Stoeckli, *Electrochim. Acta* 52 (2007) 3207.
- [13] J.A. Fernández, T. Morishita, M. Toyoda, M. Inagaki, F. Stoeckli, T.A. Centeno, *J. Power Sources* 175 (2008) 675.
- [14] J. Chmiola, G. Yushin, Y. Gogotsi, C. Portet, P. Simon, P.L. Taberna, *Science* 313 (2006) 1760.
- [15] M. Arulepp, J. Leis, M. Lätt, F. Miller, K. Rumma, E. Lust, A.F. Burke, *J. Power Sources* 162 (2006) 1460.
- [16] J. Leis, M. Arulepp, A. Kuura, M. Lätt, E. Lust, *Carbon* 44 (2006) 2122.
- [17] J. Huang, B.G. Sumpter, V. Meunier, *Angew. Chem. Int. Ed.* 47 (2008) 520.
- [18] J. Leis, A. Perkson, M. Arulepp, M. Käärik, G. Svensson, *Carbon* 39 (2001) 2043.

- [19] S. Urbonaite, J.M. Juárez-Galán, J. Leis, F. Rodríguez-Reinoso, G. Svensson, *Microp. Mesop. Mater.* (2008, In press)
- [20] J. Leis, M. Arulepp, M. Lätt, H. Kuura, PCT Patent WO 11847, 2005
- [21] F. Rouquérol, L. Luciani, Ph. Llewellyn, R. Denoyel, J. Rouquérol, In : *Traité d'Analyse et Caractérisation-Texture des matériaux pulvérulents*. Editions Techniques de l'Ingénieur, Paris, 2004, p 1-24.
- [22] F. Stoeckli, T.A. Centeno, *Carbon* 43 (2005) 1184.
- [23] M.V. López-Ramón, F. Stoeckli, C. Moreno-Castilla, F. Carrasco-Marín, *Langmuir* 16 (2000) 5967.
- [24] F. Carrasco-Marín, A. Mueden, T.A. Centeno, F. Stoeckli, C. Moreno-Castilla, *J. Chem. Soc. Faraday Trans.* 93 (1997) 2211.
- [25] T.A. Centeno, J.A. Fernández, F. Stoeckli (2008, In press).
- [26] F. Stoeckli, A. Lavanchy, *Carbon* 38 (2000) 475.
- [27] F. Stoeckli, T.A. Centeno, *Carbon* 35 (1997) 1097.
- [28] G. Lota, T.A. Centeno, E. Frackowiak, F. Stoeckli, *Electrochim. Acta* 53 (2008) 2210.
- [29] M. Arulepp, L. Permann, J. Leis, A. Perkson, K. Rumma, A. Jänes, E. Lust, *J. Power Sources* 133 (2004) 320.

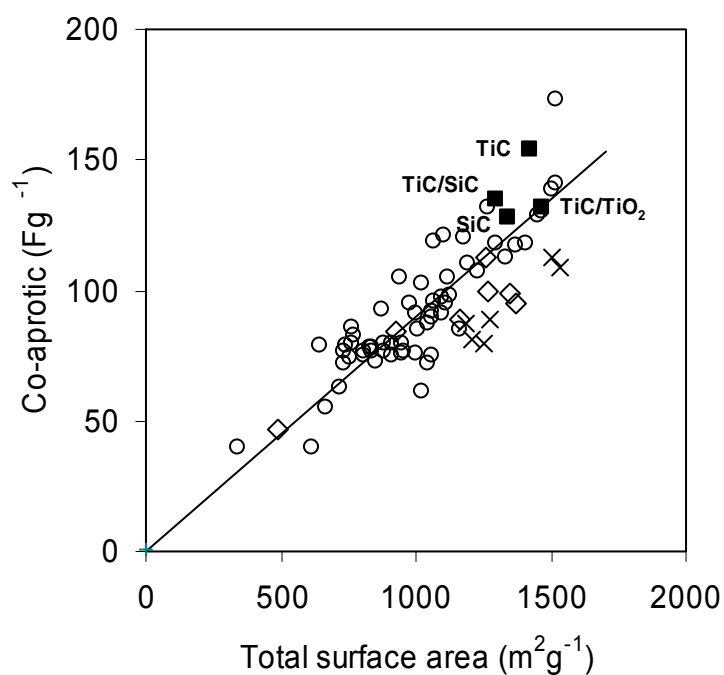


Figure 1. Variation of the limiting gravimetric capacitance at 1 mA cm⁻² in (C₂H₅)₄NBF₄/acetonitrile with the total surface area of carbide-derived carbens (■), activated carbons [6-8] (○), mesoporous templated carbons [12] (x) and mesoporous carbons obtained from the carbonization of PVA/MgO mixtures [13] (◇). The line through the origin corresponds to a linear best fit for activated carbons. The capacitance corresponds to the carbon mass in a single electrode

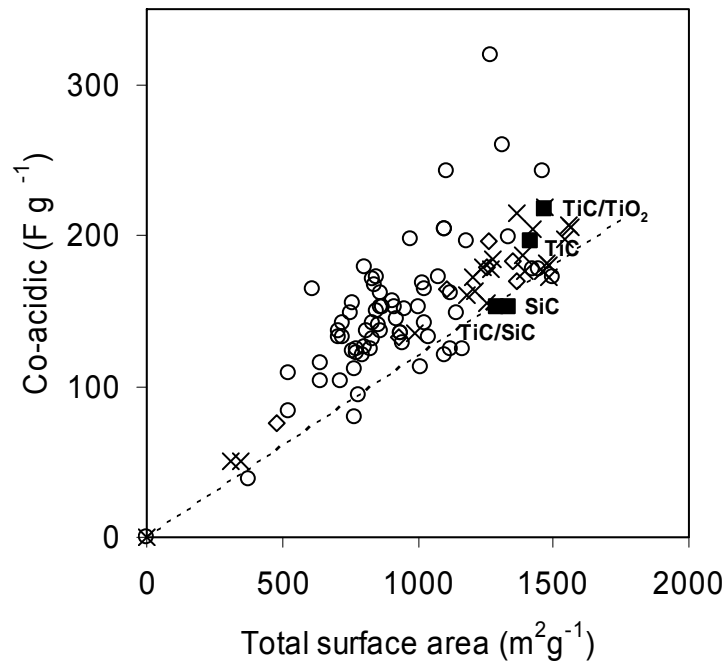


Figure 2. Variation of the limiting gravimetric capacitance at 1 mA cm⁻² in the acidic electrolyte, with the total surface area of carbide-derived carbons (■), activated carbons [6-8] (○), mesoporous templated carbons [12] (x) and mesoporous carbons obtained from the carbonization of PVA/MgO mixtures [13] (◇). The dotted line corresponds ideally to carbons with low surface oxygen (0.12 F m⁻²). The capacitance refers to the carbon mass in a single electrode.

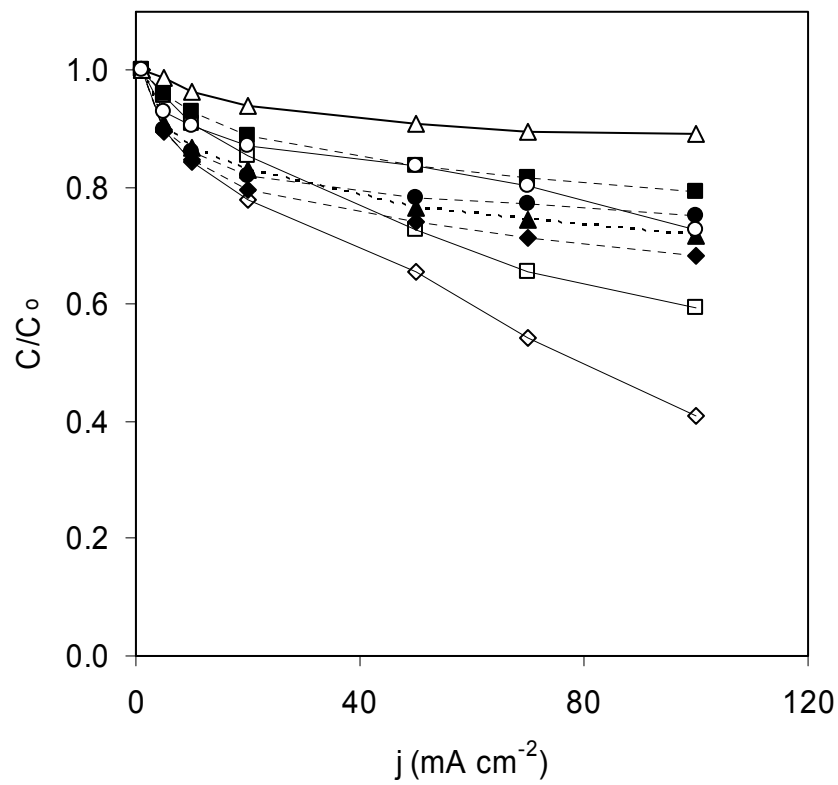


Figure 3. Variation of the relative capacitance C/C_0 with the current density j for CDCs TiC (●), TiC/SiC (■), SiC (▲), TiC/TiO₂ (◆), activated carbons AU-46 (○), MX-3 (□), Maxsorb (◇) and mesoporous carbon (Δ) in the aqueous H₂SO₄ electrolyte.

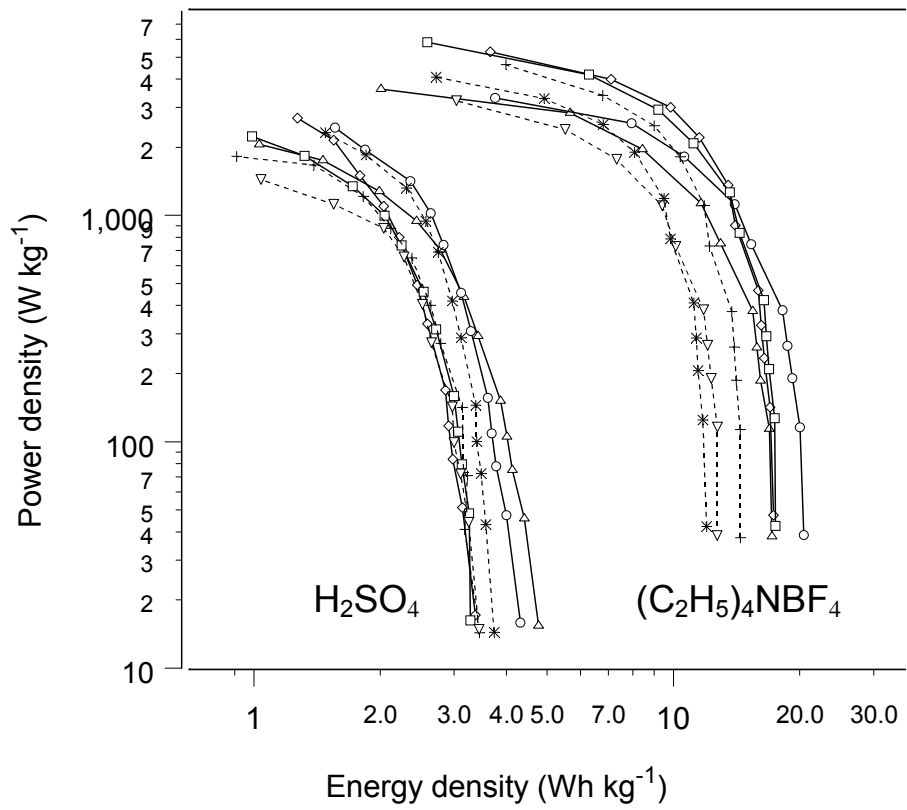


Figure 4. Ragone-type plots for carbide-derived carbons: TiC (○), TiC/SiC (□), TiC/TiO₂ (Δ), SiC (◇), commercial activated carbons for supercapacitors: Super DLC-30 (▽), Picactiv SC (+) and mesoporous carbon: MP-55 [13] (*).

The data correspond to the carbon mass in the capacitor

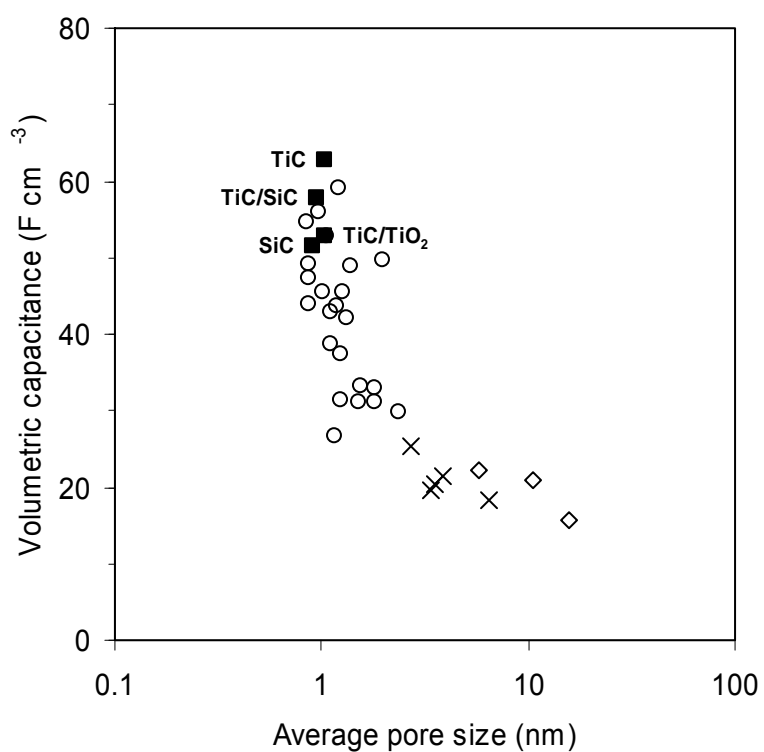


Figure 5. Evolution of the volumetric capacitance of the electrode at 1 mA cm^{-2} in $1 \text{ M } (\text{C}_2\text{H}_5)_4\text{NBF}_4/\text{acetonitrile}$ with the average pore size of CDC materials (■), typical activated carbons [6-8] (○), mesoporous templated carbons [12] (x) and mesoporous carbons derived from the carbonization of PVA/MgO mixtures [13] (◇). The values correspond to the capacitance and the volume of a single electrode.

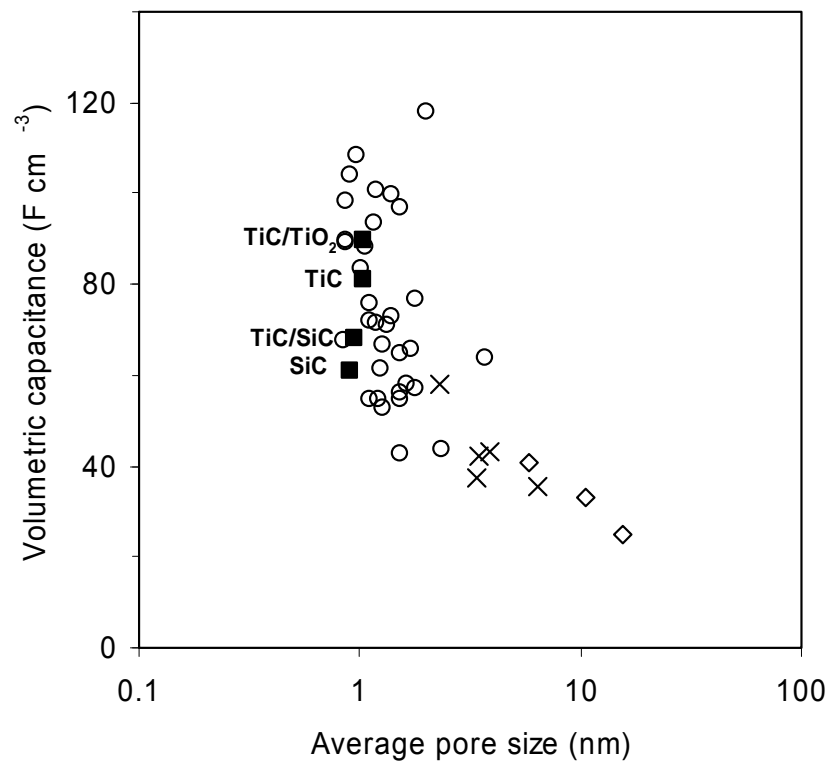


Figure 6. Evolution of the limiting volumetric capacitance of the electrode at 1 mA cm^{-2} in $2\text{M H}_2\text{SO}_4$ aqueous electrolyte with the average pore size of CDC materials (■), typical activated carbons [6-8] (○), mesoporous templated carbons [12] (x) and mesoporous carbons from the carbonization of PVA/MgO mixtures [13] (◇). The values correspond to the capacitance and the volume of a single electrode.

Table 1. Textural and chemical properties for the carbide-derived carbons.

Carbon	V _p (cm ³ g ⁻¹)	W _o (cm ³ g ⁻¹)	L _o (nm)	S _{mi} (m ² g ⁻¹)	S _{ext} (m ² g ⁻¹)	S _{total} (m ² g ⁻¹)	S _{comp} (m ² g ⁻¹)	S _{BET} (m ² g ⁻¹)	-Δ _i H(C ₆ H ₆) (J g ⁻¹)	-Δ _i H(H ₂ O) (J g ⁻¹)	-Δ _i H(CCl ₄) (J g ⁻¹)	-h _i (H ₂ O) (J m ⁻²)
SiC	0.62	0.58	0.90	1289	50	1339	1218	1234	182.7	26	177.6	0.020
TiC/SiC	0.66	0.60	0.94	1277	18	1295	1273	1337	201.6	42	205.7	0.032
TiC/TiO ₂	0.86	0.75	1.03	1456	12	1468	1389	1708	207.2	72	-	0.049
TiC	0.82	0.73	1.04	1404	15	1419	1401	1627	218.2	59	192.7	0.041

V_p = total pore volume

W_o = micropore volume

L_o = average micropore width

S_{mi} = microporous surface area

S_{ext} = external (non-microporous) surface area

S_{total} = total surface area obtained from S_{mi} + S_{ext}

S_{comp} = total surface area estimated from comparison plot

S_{BET} = total surface area obtained from BET-equation

-h_i(H₂O) = -Δ_iH[H₂O] / S_{total}

Table 2. Electrochemical properties for the carbide-derived carbons.

Carbon	$(C_2H_5)_4NBF_4/$ acetonitrile				H_2SO_4				$C_{O-aprotic} / C_{O-acidic}$
	$C_{O-aprotic}$			C_{50}/C_o	$C_{O-acidic}$			C_{50}/C_o	
	$F g^{-1}$	$F m^{-2}$	$F cm^{-3}$		$F g^{-1}$	$F m^{-2}$	$F cm^{-3}$		
SiC	129	0.096	51.4	0.90	153	0.114	61.0	0.80	0.84
TiC/SiC	130	0.100	57.7	0.89	153	0.118	67.9	0.86	0.85
TiC/TiO ₂	128	0.087	52.8	0.84	217	0.148	89.5	0.77	0.59
TiC	152	0.107	62.7	0.85	196	0.138	80.9	0.81	0.78